Increasing the synthesis/hydrolysis ratio of aminoacylase 1 by site-directed mutagenesis

Wardenga, Rainer; Lindner, Holger A.; Hollmann, Frank; Thum, Oliver; Bornscheuer, Uwe

Publisher's version / Version de l'éditeur:
https://doi.org/10.1016/j.biochi.2009.09.017
Biochimie, 91, 1, pp. 102-109, 2010-01-01

Biochimie 92 (2010) 102–109

Contents lists available at ScienceDirect

Biochimie

journal homepage: www.elsevier.com/locate/biochi

Research paper

Increasing the synthesis/hydrolysis ratio of aminoacylase 1 by site-directed mutagenesis

Rainer Wardenga [a], Holger A. Lindner [b], Frank Hollmann [c,1], Oliver Thum [c], Uwe Bornscheuer [a,*]

[a] Institute of Biochemistry, Dept. of Biotechnology & Enzyme Catalysis, Greifswald University, Felix-Hausdorff-Str. 4, D-17487 Greifswald, Germany
[b] Biotechnology Research Institute, National Research Council of Canada, 6100 Royalmount Avenue, Montréal, Québec H4P 2R2, Canada
[c] Evonik Goldschmidt GmbH, Goldschmidtstrasse 100, 45127 Essen, Germany

ARTICLE INFO

Article history:
Received 10 July 2009
Accepted 30 September 2009
Available online 9 October 2009

Keywords:
Aminoacylase
Pig kidney
Computer modeling
N-acyl-L-amino acids

ABSTRACT

Aminoacylase-1 from pig kidney (pAcy1) catalyzes the highly stereoselective acylation of amino acids, a useful conversion for the preparation of optically pure N-acyl-L-amino acids. The kinetic of this thermodynamically controlled conversion is determined by maximal velocities for synthesis (V_{mS}) and hydrolysis (V_{mH}) of the N-acyl-L-amino acid. To investigate which parameter affects maximal velocities, we focused on the proton acceptor potential of the catalytic base, E146, and studied the influence of the active site architecture on its contribution to the pKa of residue E146. The modeled structure of pAcy1 identified residue D346 as having the strongest impact on the electrostatic features of the catalytic base. Substitutions of D346 generally decreased enzymatic activities but also altered both the pH-dependency of hydrolytic activity and the V_{mS}/V_{mH} ratio of pAcy1. A reduced theoretical pKa value and a lowered experimental pH optimum of hydrolytic rates for the D346A mutant were associated with a 9-fold increase in V_{mS}/V_{mH}. This supports the importance of electrostatic contributions of D346 to the acid-base properties of E146 and demonstrates for the first time the possibility of engineering the V_{mS}/V_{mH} ratio of pAcy1.

1. Introduction

The use of hydrolytic enzymes as catalysts in organic synthesis is widespread. Applications of these enzymes in reverse hydrolysis reactions often relies on their stability in non-aqueous solvents that favor product formation [1,2]. Random approaches to optimize hydrolases for such applications, e.g. error-prone PCR, necessitate the construction of large libraries and thus require efficient selection or screening strategies to identify clones with desired properties. In the absence of such strategies, available structure-function information may guide the improvement of library quality and hence decrease the library size. For processes in aqueous systems, optimization or even reversal of enzymatic synthesis over hydrolysis ratios has been achieved for reactions involving an acyl-enzyme intermediate using e.g., penicillin acylases or glycosyl enzymes by semi-random approaches [3,4]. Yet, optimization of hydrolytic enzymes not forming a covalent intermediate has remained a considerable challenge. As an example, mutation of a non-essential histidine to aspartate in the active site of chicken creatinine kinase abolished the enzyme's hydrolytic activity while maintaining 1.6% of its synthetic activity (ATP-synthesis), presumably, through alterations in the electrostatic environment of the active site [5]. This demonstrates that engineering of the ratio of maximal velocities for synthesis and hydrolysis in the absence of a covalent reaction intermediate is also attainable.

N-acyl-L-amino acid amidohydrolases (Aminoacylases, EC 3.5.1.14) from mammalian tissues [6], plants [7] and microorganisms [8,9] allow a broad spectrum of applications in biocatalysis. Due to their exquisite stereoselectivity they are frequently used as catalysts for the kinetic resolution of racemic N-acyl-D,L-amino acids [10] but also in synthetic applications by reversal of the hydrolytic reaction [11–13]. The advantage of an aminoacylase-catalyzed process consists of the possibility to obtain the desired N-acyl-L-amino acid directly in a single step from the corresponding free L-amino acid and acyl donor, respectively. Strategies to facilitate this reaction for certain amino acid and acyl donor combinations include the use of water miscible solvents in combination with an excess of one substrate and continuous precipitation of the product [12–14]. Aminoacylase-1 from pig kidney (pAcy1) displays a marked preference for short-chain acyl moieties and non-branched aliphatic L-amino acids [15,16] and has gained considerable attention as chiral catalyst. A number of studies have reported on the use of pAcy1 in reverse hydrolysis, e.g., in the synthesis of short-chain and surface-active amphipathic N-acyl-L-amino acids. The reaction, however, has an unfavorable equilibrium

* Corresponding author. Tel.: + 49 3834864367; fax: +49 3834 86 80066.
E-mail address: uwe.bornscheuer@uni-greifswald.de (U. Bornscheuer).
[1] Present address: Biocatalysis and Organic Chemistry, Delft University of Technology, Department of Biotechnology, Julianalaan 136, 2628 BL Delft, Netherlands.

0300-9084/$ – see front matter © 2009 Elsevier Masson SAS. All rights reserved.
doi:10.1016/j.biochi.2009.09.017

in water and proceeds at a low catalytic rate [14,17–19]. Synthesis of N-acetyl-L-methionine (A-L-Met) by pAcy1 was shown to be most efficient at pH 6 while hydrolysis prevails at higher pH [17,20]. Yet, a decreased concentration of the nucleophilic free amine and thus reduced overall synthetic rates, as well as low enzyme stability precluded robust processes at the acidic pH [21].

pAcy1 belongs to the M20 family of the MH clan of co-catalytic metallopeptidases [22]. The enzyme is a homodimer with a molecular mass of 90 kDa [15] and follows a zinc-based, general base-like catalytic mechanism [23]. As a special feature of the M20 family of homodimeric enzymes, the active site in pAcy1 is situated at the subunit interface [23,24]. N-acyl-L-amino acid binding to the enzyme places the scissile bond of the substrate in the vicinity of a zinc-bound water molecule. Nucleophilic attack of this water on the amide carbonyl group is facilitated through its deprotonation by the catalytic base E146 leading to formation of a tetrahedral transition state intermediate. This collapses and releases the free amino acid and carboxylic acid. The E146-initiated water activation is thought to be the overall rate-limiting step of pAcy1-catalyzed hydrolysis [25]. The relation between the enzyme's backward and forward maximal velocities, dissociation constants and the equilibrium constant of the reaction can be described by the Haldane equation [25,26] (Equation (1)). We hypothesized that relative populations of enzyme substrate complexes are influenced by the potential of E146 to build the H-bound between the zinc coordinated water hydrogen (expressed by its pKa) and the dissociation constants of intermediates. Hence, the proton donor/acceptor potential of the catalytic base may influence the V_{mS}/V_{mH} ratio of pAcy1 and a decrease in the pKa by mutational modification of its electrostatic interactions may be a means to increase the V_{mS}/V_{mH} ratio of pAcy1. In order to achieve this, we constructed a structural homology model of pAcy1 from which computational pKa predictions identified D346 as a major determinant of E146 basicity and subjected both residues to site-directed mutagenesis followed by investigation of the properties of the mutants.

$$K_{eq} = \frac{A_{H,max} \cdot K_{Ac} \cdot K^{Ac}_{L\text{-}Am}}{A_{S,max} \cdot K_{Ac\text{-}L\text{-}Am}} \quad (1)$$

Equilibrium condition of aminoacylase 1 catalyzed reaction (Haldane relation) according to Biselli (1992) [26], see also Supplementary material, Equation S1. K_{eq} = equilibrium constant, $A_{H,max}$ = Maximum activity of the hydrolysis of N-acyl-L-amino acid, K_{Ac} = Dissociation constant of the enzyme substrate complex with the acyl compound, $K^{Ac}_{L\text{-}Am}$ = Dissociation constant of the enzyme (Ac)(L-Am) substrate complex with release of amino acid, $A_{S,max}$ = Maximum activity of the synthesis of N-acyl-L-amino acid, $K_{Ac\text{-}L\text{-}Am}$ = Dissociation constant of the enzyme substrate complex with N-acyl-L-amino acid.

2. Material and methods

Unless stated otherwise chemicals were purchased from Fluka (Buchs, Switzerland), Sigma (Steinheim, Germany) and Merck (Darmstadt, Germany) at the highest purity available. *Escherichia coli* BL21 (DE3) (Invitrogen, Carlsbad, USA) [F− ompT hsdSB(rB − mB −) gal dcm rne131(DE3) was used for protein expression. *E. coli* DH5α (Clontech, Saint-Germain-en-Laye, France) [supE44ΔlacU169 (Φ80lacZΔM15) hsdR17 recA1 endA1 gyrA96 thi-1relA1] was used for cloning.

2.1. Modeling of pAcy1 catalyzed N-acylation

The published kinetic model of aminoacylase 1 [25,26] was used for theoretical investigation of the influence of rate constants on the kinetic of the N-acylation (Supplementary material, Equation S1). The equation was implemented in a computable script using MATLAB 6.5 (MathWorks Inc., Natick MA, USA) and calculations for equilibrium conversion were performed using published parameters for the synthesis and hydrolysis of N-acetyl-L-alanine [25,26] with variations in the V_{mS}/V_{mH} ratio, dissociation constants and enzyme concentration.

2.2. Homology modeling

The pAcy1 homology model was build with the program MODELLER 9V4 (http://salilab.org/modeller/) as described previously by Liu et al. [27] with slight modifications and with additional analysis of topological errors and energy minimization as described in Supplementary material.

2.3. Web-based computational prediction of pKa values

Estimation of pKa values and significant contributions of neighboring groups on the protonation state of E146 were extracted from results of the H++ web server [28–30] (http://biophysics.cs.vt.edu/H++/) using homology models of wild-type and mutant pAcy1 enzymes. All protonation states were calculated by solving finite difference Poisson–Boltzmann equation for pH 7.5 using the following physical conditions: salinity, 0.15; internal dielectric, 6; external dielectric, 80.

2.4. Recombinant DNA technologies

All routine DNA technologies were performed according to standard protocols [31]. Restriction enzymes and other DNA-modifying enzymes were used as specified by the suppliers (New England Biolabs, Beverly, MA, USA; Promega, Madison, WI, USA). DNA-sequencing reactions were carried out at GATC-Biotech (Konstanz, Germany). Standard protocols were used for the preparation and transformation of competent *E. coli* cells [32].

2.5. Site-directed mutagenesis

Site-directed mutagenesis was performed on the expression vector pET-52(b) containing the pAcy1 gene [33] using the QuikChange™ site-directed mutagenesis kit (Stratagene, Heidelberg, Germany). Forward versions of mutagenic primers are listed in Table 1. *Dpn*I-treated DNA was transformed into electro-competent *E. coli* DH5α cells and mutations were confirmed by DNA sequencing. For expression, competent *E. coli* BL21 (DE3) cells harboring the chaperone co-expression vector pTf16 (Takara Bio, Otsu, Shiga, Japan) were transformed with mutated plasmid.

2.6. Expression and purification

pAcy1 and its variants were expressed in *E. coli* BL21 (DE3) and purified as described before [33]. In brief, 50 mL cultures of *E. coli*

Table 1
Forward primers.

Mutant	Oligonucleotide sequence[a]
E146A	5′-CC TTT GTG CCG GAT GCG GAA GTG GGC GGC-3′
E146D	5′-CC TTT GTG CCG GAT GAT GAA GTG GGC GGC-3′
E146Q	5′-CC TTT GTG CCG GAT CAG GAA GTG GGC GGC CA-3′
E146N	5′-CC TTT GTG CCG GAT AAC GAA GTG GGC GGC-3′
D346A	5′-CCG GCG AGC ACC GCG GCG CGT TAT ATT CGT-3′
D346Q	5′-CCG GCG AGC ACC CAG GCG CGT TAT ATT CG-3′
D346N	5′-CCG GCG AGC ACC AAC GCG CGT TAT ATT CGT-3′
D346E	5′-CCG GCG AGC ACC GAA GCG CGT TA

[a] Altered nucleotides, which introduced the desired mutations, are underlined.

cells were harvested 24 h after induction of pET52(b)+ harboring a codon-optimized pAcy1 gene. The molecular chaperone trigger factor was co-expressed from the beginning of the cultivation from plasmid pTf-16 (Takara Bio, Otsu, Shiga, Japan) by induction with arabinose (1 mg/ml). Cells were disrupted by sonification, and the enzyme was purified by StrepTag chromatography (IBA, Göttingen, Germany) according to the manufacturers protocol but without EDTA containing buffers. Enzyme preparations were stored with 50% glycerol at −20 °C. No loss of activity was observed for activity measurements within 4 weeks.

2.7. Protein assays

Protein concentrations were determined by the BCA-assay (Uptima Interchim, France) using BSA as standard. SDS-PAGE was performed in 12% (w/v) polyacrylamide gel with a stacking gel (4%) as described by Laemmli to check the purity and the molecular mass [34]. The proteins in the low-molecular-weight standard mixture obtained from Roth (Roti®-Mark STANDARD) or IBA (Strep-tag® Protein Ladder) were used as reference.

2.8. Circular dichroism spectra

Buffer exchanges for purified enzymes to 5 mM sodium phosphate buffer pH 7.5 were done using NAP-5 columns (GE Healthcare Bio-Sciences, Freiburg, Germany). The Near-UV CD spectra of pAcy1 variants were recorded at 20 °C in a JASCO J-810 circular dichroism spectropolarimeter under nitrogen using 0.06 mg/ml of protein, a sample cell path length of 2 mm, and response time and band width of 1 s and 1 nm, respectively. Ten scans between 190 and 270 nm were averaged to ensure a good signal-to-noise ratio.

2.9. Aminoacylase assays

pAcy1 variants at concentrations ranging from 0.5 to 1 mg/ml were incubated at 25 °C in a 50 mM sodium phosphate buffer, pH 7.5, in the presence of 300 mM L-methionine and 30 mM acetate for measurements of A-L-Met synthesis [17] and of 20 mM A-L-Met for hydrolysis studies. For controls, enzyme was omitted from these mixtures. Per reaction, five samples were withdrawn and quenched by adding 6 N HCl at defined intervals over reaction times ranging from 5 min to 24 h. A-L-MET in these aliquots was separated and quantified by reverse phase high performance liquid chromatography (HPLC) (MERCK-HITACHI, Tokyo, Japan) on a Kromasil C8 column (4.0 × 60 mm, particle size 5 μm, SYNTREX GbR, Greifswald, Germany) using isocratic elution with 95% H_2O, 5% (v/v) acetonitrile and 0.01% (v/v) trifluoroacetic acid. The retention time of A-L-MET, monitored at 214 nm, was 1.1 min at a flow rate of 4.5 ml/min. Initial rates were determined from peak areas by linear regression using Origin Pro 7.5 software (Northampton, MA, USA). V_{mS}/V_{mH} ratios were determined and averaged from three independent preparations of each variant. One unit (U) of pAcy1 activity was defined as the amount of enzyme that hydrolyzes 1 μmol of A-L-Met per minute.

The pH-dependencies of enzymatic hydrolysis were assayed spectrophotometrically with 3-(2-furyl)acryloyl-L-methionine (FA-L-Met) as a substrate at 25 °C. Chemical synthesis of FA-L-Met and the assay were performed according to Giardina et al. [35]. A standard reaction mixture of 100 μl contained 5 ng of enzyme and 1.2 mM FA-L-Met in a 20 mM MES-NaOH buffer. In the investigated pH range of 4.5–7.2, FA-L-Met showed no significant change in absorption, and the addition of NaOH affected the ionic strength negligibly with Δ 15 mM from pH 5.5 to pH 7.2. Measurements were set up in quadruplicate on 96-well plates with 5 μl of enzyme (1 mg/ml) and 95 μl of pH-adjusted FA-L-Met stock solution (pH 4.5, 5.0, 5.5, 5.8, 6.0, 6.5, 6.7, 6.9, 7.2) per well. Changes in absorption over time were recorded in a Varioscan microplate reader (Thermo Electron Corporation, USA) and were evaluated by regression analysis of the linear interval using Origin Pro 7.5. Due to variations in absolute activities measured for mutants from individual preparations, pH-dependent activities were normalized to percent of maximum. Resulting standard errors of the mean were within 3%. Origin Pro 7.5 was used for sigmoidal data fitting.

3. Results

In order to understand the parameters influencing the V_{mS}/V_{mH} ratio of pAcy1-catalyzed reactions, we analyzed the contribution of the active site architecture to the pKa of E146 and applied site-directed mutagenesis to the most important residues E146 and D346 as outlined in the next paragraphs.

3.1. Modeling of pAcy1 catalyzed N-acylation

According to the kinetic model of pAcy1 catalysis by Biselli (1992) [25,26], maximal velocities and the enzymatic V_{mS}/V_{mH} ratio determines the time needed to reach equilibrium conversion (Supplementary material, Equation S1). Model-based simulations suggest that an increase of V_{mS} by a factor of two at constant V_{mH} can speed up attainment of the reaction equilibrium by approximately the same time as a doubling of the amount of enzyme (Supplementary material, Fig. S1).

3.2. Homology modeling

Detailed procedures for the building of structural models for wild-type and mutant pAcy1 are given in Supplementary material. The procedure was exhaustively validated and homology models of wild-type pAcy1 were verified for structural integrity. The most reliable model underwent an energy minimization procedure and a molecular dynamic simulation for 500 ps. After this, the PROCHECK overall average G factor, which checks the stereochemical quality and overall structure geometry, was 0.10 with a score less than −0.5 indicating a poor model. ERRAT was used for identifying incorrectly folded regions and the calculated overall quality factor of 92.9, was well within the range of a high quality model (factor >50). Thus, the backbone conformation and non-bonded interactions of the homology model are all within a reasonable range. Using VERIFY-3D for evaluation of compatibility between the amino acid sequence and the environment of the amino acid side chains, 84.28% of the residues had a 3D-1D score of >0.2 indicating the good compatibility of each amino acid residue in the local 3D structure. Individual examinations of residues with a distance of 8 Å to the catalytic base indicated no structural errors in the active site (data not shown). Derived structures of D346N, D346Q, D346E and D346A variants showed only minor variations in overall and individual residue quality scores.

3.3. Local electrostatic environment of E146 and pKa predictions

We used our homology model of pAcy1 to study the importance of the local electrostatic environment on the acid-base properties of the enzyme's putative catalytic base residue E146. H++ calculations resulted in a pKa_{E146} of 5.8. The H++ server identified 17 pH-independent contributions of non-titratable groups (background) and 10 pH-dependent direct interactions of titratable groups with E146, four of which involve zinc ligands (Supplementary material, Table SI) (Fig. 1). Background contributions ranged between −1.76 and 0.65 with a sum of 4.2 and a mean of −0.25 (±0.07). Direct contributions ranged between −0.6 and 2.18 with a sum of +7.5 and a mean of +0.86 (±0.27). Although a background contribution of 1.76 from T345 was the highest above the mean, the strongest individual direct influence on pKa_{E146} was predicted for D346

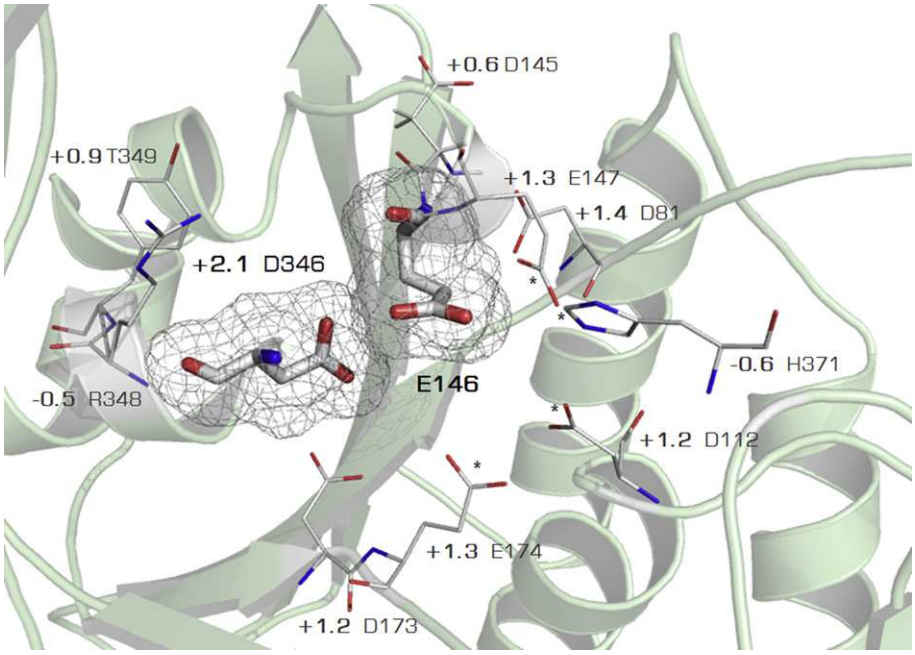

Fig. 1. Significant contributions to the pKa of E146 by interactions with titratable neighboring groups in the pAcy1 homology model. The protein backbone is shown as green ribbon, residue side chains are shown with lines and a surface mesh for residues E146 and D346, respectively, is shown in grey. Zinc-binding residues are each marked with an asterisk. The model was drawn with PYMOL V1.1 [42]. (For interpretation of the references to colour in this figure legend, the reader is referred to the web version of this article.).

(+2.18), which is located 4.5 Å from the catalytic base. In the refined crystal structure of human Acy1 (hAcy1), the conserved D346 (D348 in hAcy1) is located 4.6 Å from the catalytic glutamate, also supporting an electrostatic interaction. Electrostatic calculations for models of the D346N, D346Q, D346E, and D346A mutants of pAcy1 (Supplementary material, Fig. S2) suggested, that only the alanine variant reduced the basicity of E146 from a pKa of 5.8 to 5.1, whereas the asparagine, glutamine, and glutamate variants increased this value by 0.3, 1.5, and 3.3 units, respectively (Table 2).

3.4. Expression & characterization of pAcy1 variants

Based on the results of the computational analysis, the following mutants were constructed and expressed in *E. coli*: E146A, E146D, E146Q, E146N, D346E, D346A, D346Q, and D346N. All mutants of pAcy1 generated in this work showed the same expression and purification behavior as the wild-type enzyme with only minor differences in protein yield (Fig. 2). CD spectra of pAcy1 and its mutants suggested the presence of well-folded proteins in all cases and only a very slight decrease in α-helix for E146N (Fig. 3). Hydrolytic activity of wild-type pAcy1 against A-L-Met was ~77 U/mg and the synthesis activity was quantified to ~2.9 U/mg resulting in a V_{mS}/V_{mH} ratio of 37×10^{-3}. Catalytic activities of all mutants were significantly decreased but more for variation of E146 than of D346. In the case of the E146 variants, residual activities at pH 7.5 did not exceed 0.39 U/mg for hydrolysis (E146D) and 4.6 mU/mg for synthesis (E146A) but no significant shift in the V_{mS}/V_{mH} ratio was observed (data not shown).

Mutation of D346 also significantly reduced the rates of both A-L-Met synthesis and hydrolysis at pH 7.5 (Fig. 4A). Compared to wild-type pAcy1 catalytic rates, the D346E and D346N mutants showed two, and the D346Q and D346A mutants showed three orders of magnitude reductions in synthesis. While D346E, D346N, and D346Q displayed only between 10- and 25-fold reductions for hydrolysis, this activity was reduced even 4000-fold with the D346A variant. V_{mS}/V_{mH} ratios were thus decreased about 5-, 8-, and 15-fold for D346E, D346N, and D346Q, respectively, but in contrast showed an approximately 9-fold increase for D346A (Fig. 4B, Table 2).

Mutants of D346 showed bell-shaped pH-dependencies of maximum catalytic activities towards FA-L-Met (Fig. 5), with the exception of D346E which showed a distinct shift to more basic values. Mutation of D346 to either asparagine or glutamine had only minor effects on the pH-dependencies, whereas mutation to alanine produced a narrower pH-profile and shifted the pH optimum of hydrolysis towards more acidic values by −1.02 units (Table 2).

Table 2
Summary of the effects of D346 substitutions in pAcy1.

pAcy1 variant	ΔpKa E146[a]	V_{mS}/V_{mH} ratio[b] (fold change)	pH optimum[c]
D346[d]	–	–	7.2
D346Q	+1.5	15× ↓	6.8
D346N	+0.3	8× ↓	7.2
D346E	+3.3	5× ↓	>7.2
D346A	−0.7	9× ↑	6.18

[a] Calculated values.
[b] V_{mS}/V_{mH} ratios are given for A-L-Met.
[c] pH optima are given for maximal rates of FA-L-Met hydrolysis ($n = 3$).
[d] The theoretical pKa of E146 in the wild-type enzyme is 5.8, and the V_{mS}/V_{mH} ratio of 0.037.

4. Discussion

Acy1 from porcine kidney has been considered as a biocatalyst for the aqueous one-step synthesis of short-chain and surface-active amphipathic N-acyl-L-amino acids [14,17–19]. Our simulation of the pAcy1-catalyzed amino acid N-acylation reaction based on the kinetic model by Biselli (1992) (Supplementary material, Equation S1 and Fig. S1) suggests that, with constant reaction time and product yield, a twofold increase in the V_{mS}/V_{mH} ratio obtained by an increase of V_{mS} at constant V_{mH} potentially affords a twofold reduction in the amount of enzyme applied. Therefore and in light of the known limitations of K_{cat}/K_M as a measure of catalytic efficiency for synthesis

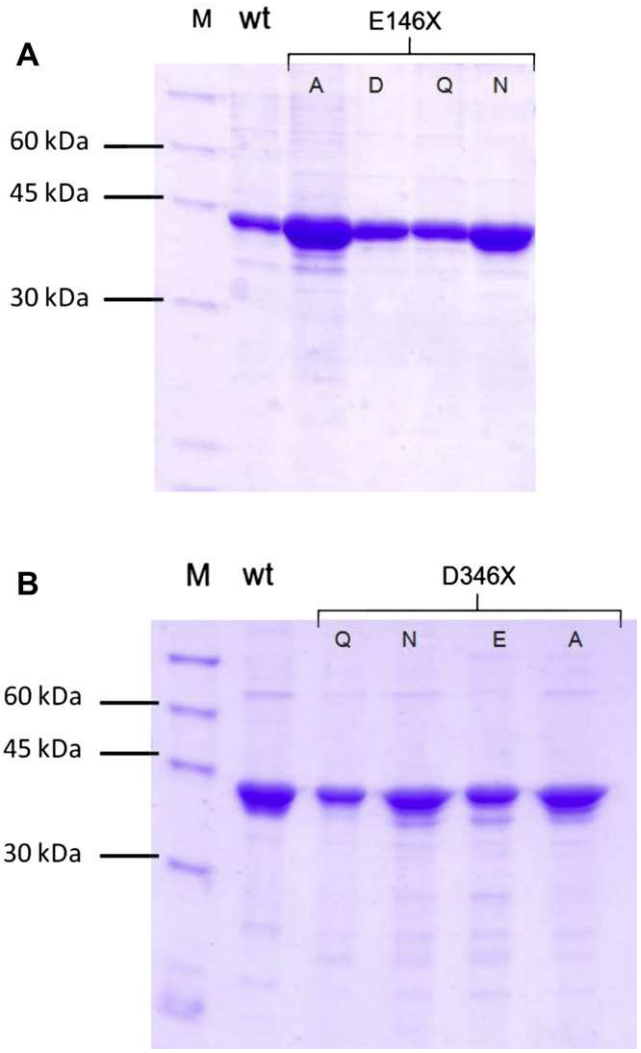

Fig. 2. SDS-PAGE analysis of fractions obtained by strep-tag purification of recombinant pAcy1 variants. M – Marker, wt – Wild-type pAcy1, (A) E146X – pAcy1 mutants of E146, (B) D346X – pAcy1 mutants of D346.

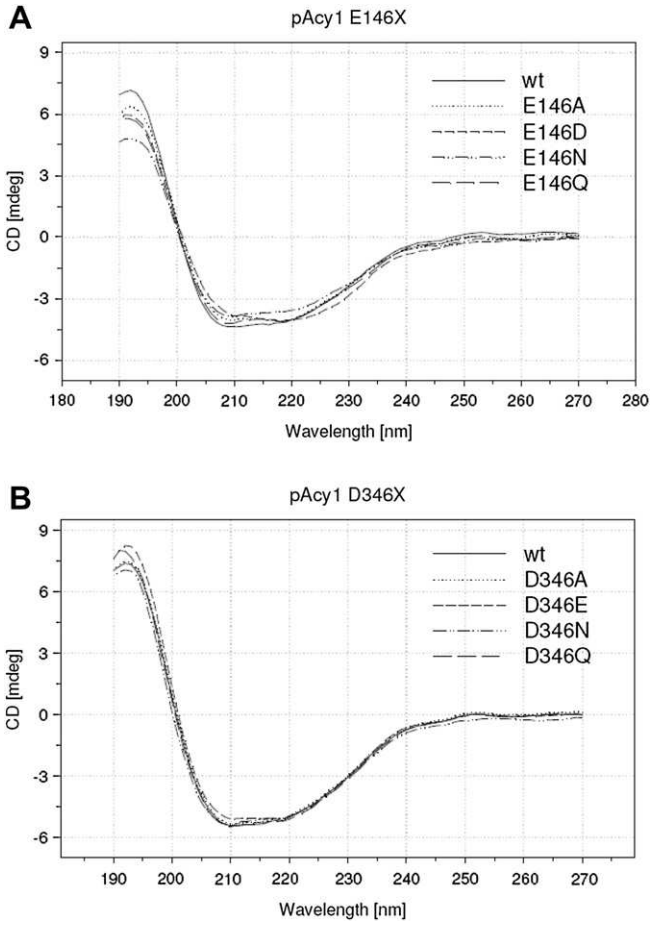

Fig. 3. CD spectra for recombinant pAcy1 mutants of (A) E146 and (B) D346 variants.

[36] we focused on determination and optimization of the enzymatic V_{mS}/V_{mH} ratio which may promote synthetic applications of pAcy1. We sought to identify residues in pAcy1 that may function as target sites for a semi-random approach to increase the V_{mS}/V_{mH} ratio of the enzyme. The enzyme follows a zinc-based, general base-like catalytic mechanism [23]. Deprotonation of a zinc-activated water by E146 generates the hydrolytic nucleophile and is thought to be the rate-limiting step of the overall reaction [25].

In line with previous mutational studies on human and rat Acy1 [23,37] mutation of the putative catalytic base residue E146 in pAcy1 to alanine, aspartate, glutamine, or asparagine reduced the specific activities for both A-L-Met hydrolysis and synthesis at least 200- and 630-fold, respectively, and did not cause clear changes in enzymatic V_{mS}/V_{mH} ratios (data not shown). With the possible exception of the E146N variant, highly similar CD spectra (Fig. 3A) indicated properly folded enzymes for all variants of E146 and suggest that reduced activities were not due to global changes in enzyme structures. In accordance with enzymatic microreversibility principles, E146 thus appears to act as an acid/base catalyst in both N-acyl-L-amino acid synthesis and hydrolysis.

We rationalized that a reduction in the basicity of E146 may yield a pAcy1 variant with potentially an improved V_{mS}/V_{mH} ratio, and that this may be achieved by altering the local electrostatic environment. In order to map electrostatic contributions in the active site of pAcy1 that determine the pKa of E146, we constructed a homology model for the catalytic domain of the enzyme based on a published procedure [27] with additional validation of structural integrity. Individual quality scores for residues within 8 Å of the catalytic base supported the accuracy of our model. Using the H++ web server, we calculated from our model a pKa for E146 of 5.8, very close to the value of 5.9 estimated by Röhm and Van Etten [18] based on pAcy1-catalyzed ^{18}O exchange between acetate and water. The H++ server identified electrostatic contributions to the pKa of E146 from both ionizable and non-ionizable groups in the enzyme active site (Supplementary material, Table SI) (Fig. 1). Amongst the 27 identified groups, the side chain of D346 contributed the strongest to a raise in the intrinsic pKa of the side chain carboxyl group of the E146 from around 4.4 [38] to a predicted value of 5.8. pKa predictions for E146 from our structural models of D346 mutants suggested that conservative substitutions, i.e., to asparagine, glutamine, and glutamate, all raise the pKa of E146 (Table 2). The comparatively high 3.3 unit raise in the pKa of E146 through the neutral asparagine to glutamate mutation is in agreement with an alkaline proximity effect of the negative charge at position 346 approaching the base residue by 1 Å [39]. Accordingly, elimination of the direct contribution of D346 through replacement of this residue by alanine is predicted to indeed lower the basicity of E146 by −0.7 pKa units. It has to be mentioned that mutations of D346 likely influence the actual pKa of E146 by mechanisms other than changes in local electrostatics, such as altered protein dynamics [39].

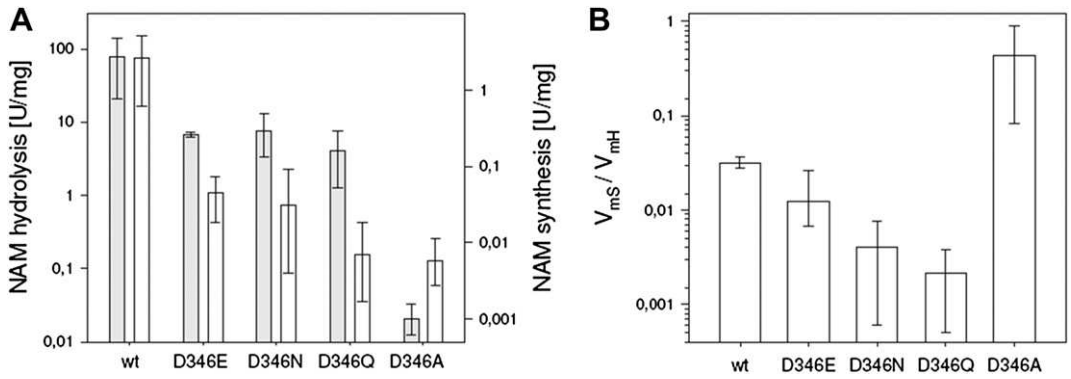

Fig. 4. N-acetyl-L-methionine (A) synthesis and hydrolysis and (B) V_{mS}/V_{mH} ratios for pAcy1 variants at pH 7.5. Means with lower and upper values are based on three parallels from independent expression and purification experiments. Gray and open bars represent hydrolytic and synthetic activities, respectively.

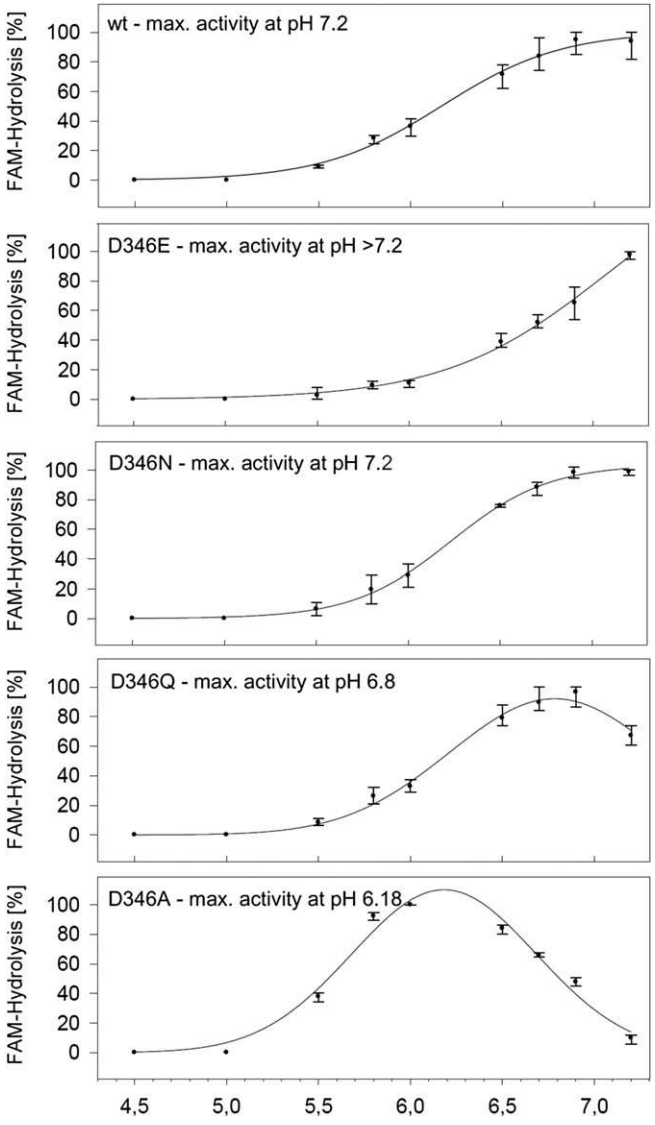

Fig. 5. Hydrolytic activities of pAcy1 variants towards FA-L-Met in dependence of pH. One representative out of three independent experiments with separate enzyme preparations is shown.

Purified asparagine, glutamine, glutamate and alanine mutants of D346 all exhibited wild-type like CD spectra (Fig. 3B) supporting the structural integrity of these pAcy1 mutants. The mutations reduced enzymatic activities at least 10-fold for hydrolysis and 60-fold for synthesis of A-L-Met (Fig. 4A). These reductions were an order of magnitude lower than with mutations of E146 and are consistent with an important local electrostatic interaction of D346 with the catalytic base residue E146 as suggested by our structural model of wild-type pAcy1 and H++ calculations based on structural models of D346 mutants (Table 2). Comparison of our pAcy1 model with the crystal structure of hAcy1 in complex with an amino acid ligand (PDB ID 1Q7L) indicated a distance of at least 6.4 Å between D346 and the substrate binding pocket. This suggests that D346 does not participate directly in substrate-binding. Although we can not exclude that mutation of this residue affected substrate binding indirectly, it is reasonable to assume that with a A-L-Met concentration of 20 mM and a corresponding half-saturation concentration (Michaelis constant, K_M) of 2.72 mM [40] hydrolysis was generally measured very close to saturating concentrations. During synthesis, an extremely high concentration for methionine of 300 mM (10-fold excess over acetate) approached the experimental limit of the assay but approximated saturation conditions as far as possible. Therefore, our measured V_{mS}/V_{mH} ratios depend on experimental conditions. Noteworthly – compared to the wild-type – V_{mS}/V_{mH} ratios for conservative mutations (D346N, D346Q, and D346E) were reduced 5- to 15-fold while pKa values for E146 were predicted to be increased by 0.3–3.3 units (Table 2). Contrarily, a by 0.7 units reduced theoretical pKa value of E146 for the D346A variant was associated with a 9-fold increase in the V_{mS}/V_{mH} ratio. These observations support our initial hypothesis that a reduction in the basicity of E146 by altering the local electrostatic environment could improve the enzymatic V_{mS}/V_{mH} ratio.

In order to measure pH-dependencies of pAcy1 activity, we resorted to a direct assay based on measuring the change in absorption at 340 nm, which could be multiplexed but has a lower sensitivity. pAcy1 was reported to exhibit a K_M value at pH 8.7 of about 0.1 mM with FA-L-Met [41]. K_M values for pAcy1-mediated A-L-Met hydrolysis in a MES-NaOH buffer reported by Henseling and Röhm [22] showed a very weak pH-dependency (variations within a range of no more than 1 mM between pH 5.5 and pH 8.5). We thus assumed, that our pH-profiles of FA-L-Met hydrolysis at 1.2. mM of substrate were not dominated by pH-effects on substrate affinities and thus largely reflect maximal velocities (Fig. 5). However, the reduced assay sensitivity and low residual activities of our mutant enzymes precluded the determinations of enzyme specificity constants (k_{cat}/K_M) against the pH and thus a reliable derivation of pKa values. Also, batch-to-batch variations rendered a comparison of

absolute enzyme activities imprecise. Hence, normalized data for representative experiments are shown in Fig. 5. The clear shift of the pH optimum for the D346E mutant to higher pH-values compared to the wild-type follows the strong calculated increase in the pKa for the catalytic base (Table 2). Mutation of D346 to asparagine and glutamine, respectively, only slightly shifted the pH-profiles to lower pH-values. The corresponding stronger reductions in the V_{mS}/V_{mH} ratios (Fig. 4B) for these two variants compared to D346E, especially for D346Q, were determined by a more pronounced loss in synthetic activity at pH 7.5 than with D346E (Fig. 4A). The same loss in synthetic activity as for D346Q was also seen for D346A. However, the profile for the D346A variant indicates a strong shift of the mutant's pH optimum by minus 1.02 units. This shift and a narrower pH-profile largely account for the mutant's three orders of magnitude loss in hydrolytic activity (Fig. 4A) mainly responsible for the 9-fold increase in its V_{mS}/V_{mH} ratio (Fig. 4B).

Our work was motivated by the rational that lowering the basicity of residue E146 of pAcy1 could improve the enzyme's V_{mS}/V_{mH} ratio. Structural homology modeling and computational pKa predictions provided theoretical evidence for a major contribution of D346 to the E146 basicity. All mutants of D346 generated exhibited only lower synthetic and hydrolytic activities. Despite good overall structural integrity, this is likely a result of multiple roles that D346 plays within the active site. For example, beyond influencing the pKa of E146, additional interactions by D346 may be important for the catalytic competency of pAcy1 e.g. significant electrostatic interactions with D173 were also indentified (data not shown). However, the fact that replacement of the D346 side chain with a methyl group (D346A) led to the most pronounced of the measured reductions in hydrolytic activity and thus improved the corresponding V_{mS}/V_{mH} ratio (Fig. 4B), is in accordance with a decrease in pKa E146 as calculated from our structural model of the mutant (Table 2). Experimental pH-dependencies of wild-type pAcy1 steady-state kinetic parameters were previously shown to be very small [21]. Despite no direct role of D346 in substrate binding can be assumed, the experimental data are not appropriate for deriving pKa values for our mutants. Nevertheless, we believe that the clear pH-shift for D346A by 1.02 pH units toward a more acidic value and corresponding sharpened pH transitions strongly argue in favor of a reduction in the pKa of a catalytic group involved in the rate-limiting step, most likely E146. To the best of our knowledge, this is the first reported alteration of the enzymatic V_{mS}/V_{mH} ratio for an aminoacylase-catalyzed reaction. Still, hurdles in preserving the absolute synthetic enzyme activity remain to be overcome for instance by a semi-rational approach to enzyme engineering with iterative saturation mutagenesis in the neighborhood of D346.

Acknowledgement

This work was supported by the "Fachagentur für Nachwachsende Rohstoffe" (FNR, Gülzow, Germany, Grant No. 22009405) and Evonik Goldschmidt GmbH. We thank Anita Gollin for chemical syntheses of FA-L-Met. This is NRCC publication no. 50656.

Appendix. Supplementary material

Supplementary data associated with this article can be found, in the online version, at doi:10.1016/j.biochi.2009.09.017.

References

[1] A.M. Klibanov, Enzymatic catalysis in anhydrous organic solvents. Trends Biochem. Sci. 14 (1989) 141–144.
[2] V.A.M.P. Koskinen, A.M. Klibanov, Enzymatic Reactions in Organic Media. Blackie, London, 1996.
[3] E.M. Gabor, D.B. Janssen, Increasing the synthetic performance of penicillin acylase PAS2 bystructure-inspired semi-random mutagenesis. Protein Eng. Des. Sel 17 (2004) 571–579.
[4] Y. Honda, M. Kitaoka, The first glycosynthase derived from an inverting glycoside hydrolase. J. Biol. Chem. 281 (2006) 1426–1431.
[5] M. Forstner, A. Müller, M. Stolz, T. Wallimann, The active site histidines of creatine kinase. A critical role of his 61 situated on a flexible loop. Protein Sci. 6 (1997) 331–339.
[6] M. Mitta, I. Kato, S. Tsunasawa, The nucleotide sequence of human aminoacylase-1. Biochim. Biophys. Acta 1174 (1993) 201–203.
[7] J.C. Lugay, J.N. Aronson, Palo Verde (*Parkinsonia aculeata* L.) seed aminoacylase. Biochim. Biophys. Acta 191 (1969) 397–414.
[8] I. Gentzen, H.G. Löffler, F. Schneider, Aminoacylase from *Aspergillus oryzae* comparison with the pig kidney enzyme. Z. Naturf. C 35 (1980) 544–550.
[9] V. Sakanyan, L. Desmarez, C. Legrain, D. Charlier, I. Mett, A. Kochikyan, A. Savchenko, A. Boyen, P. Falmagne, A. Pierard, Gene cloning, sequence analysis, purification, and characterization of a thermostable aminoacylase from *Bacillus stearothermophilus*. Appl. Environ. Microbiol. 59 (1993) 3878–3888.
[10] T. Sato, T. Tosa, Optical resolution of racemic amino acids by aminoacylase. BioprocessTechnol 16 (1993) 3–14.
[11] M.I. Youshko, F. van Rantwijk, R.A. Sheldon, Enantioselective acylation of chiral amines catalysed by aminoacylase I. Tetrah. Asymmetry 12 (2001) 3267–3271.
[12] K. Yokoigawa, E. Sato, N. Esaki, K. Soda, Enantioselective synthesis of N-acetyl-l-methionine with aminoacylase in organic solvent. Appl. Microbiol. Biotechnol. 42 (1994) 287–289.
[13] M. Koreishi, D. Zhang, H. Imanaka, K. Imamura, S. Adachi, R. Matsuno, K. Nakanishi, A novel acylase from *Streptomyces mobaraensis* that efficiently catalyzes hydrolysis/synthesis of capsaicins as well as N-Acyl-L-amino acids and N-Acyl-peptides. J. Agric. Food Chem. 54 (2006) 72–78.
[14] E. Wada, M. Handa, K. Imamura, T. Sakiyama, S. Adachi, R. Matsuno, K. Nakanishi, Enzymatic synthesis of N-acyl-l-amino acids in a glycerol-water system using acylase I from pig kidney. J. Am. Oil Chem. Soc. 79 (2002) 41–46.
[15] G.J. Palm, K.H. Röhm, Aminoacylase I from porcine kidney: identification and characterization of two major protein domains. J. Protein Chem. 14 (1995) 233–240.
[16] S.M. Birnbaum, L. Levintow, R.B. Kingsley, J.P. Greenstein, Specificity of amino acid acylases. J. Biol. Chem. 194 (1952) 455–470.
[17] A. Ferjancic-Biagini, T. Giardina, M. Reynier, A. Puigserver, Hog kidney and intestine aminoacylase-catalyzed acylation of L-methionine in aqueous media. Biocat. Biotrans 15 (1997) 313–323.
[18] K.H. Röhm, R.L. Etten, Catalysis by hog-kidney aminoacylase does not involve a covalent intermediate. Eur. J. Biochem. 160 (1986) 327–332.
[19] I. Galaev, V.K. Svedas, A kinetic study of hog kidney aminoacylase. Biochim. Biophys. Acta 701 (1982) 389–394.
[20] Y. Kimura, Y. Kobayashi, S. Adachi, R. Matsuno, Aminoacylase-Catalyzed synthesis of N-acyl amino acid from fatty acid or its ethyl ester and amino acid. in: S. Furusaki, I. Endo, R. Matsuno (Eds.), Biochemical Engineering 2001. Springer, Tokyo, 2001, pp. 109–111.
[21] J. Henseling, K.H. Röhm, Aminoacylase I from hog kidney: anion effects and the pH dependence of kinetic parameters. Biochim. Biophys. Acta 959 (1988) 370–377.
[22] N.D. Rawlings, F.R. Morton, C.Y. Kok, J. Kong, A.J. Barrett, MEROPS: the peptidase database. Nucleic Acids Res. 36 (2008) 320–325.
[23] H.A. Lindner, V.V. Lunin, A. Alary, R. Hecker, M. Cygler, R. Menard, Essential roles of zinciglation and enzyme dimerization for catalysis in the aminoacylase-1/M20 family. J. Biol. Chem. (2003) 44496–44504.
[24] H.A. Lindner, A. Alary, L.I. Boju, T. Sulea, R. Menard, Roles of dimerization domain residues in binding and catalysis by aminoacylase-1. Biochemistry 44 (2005) 15645–15651.
[25] K. Drauz, H. Waldmann, Enzyme Catalysis in Organic Synthesis. Wiley-VCH, Weinheim, 1995.
[26] M.F. Biselli, Enzyme-calalyzed racemate separation of amino acids with integrated racemization using the conversion of DL-alanine to L-alanine as an example. Ber. Forschungszent. Jülich, Jülich (1992) 192.
[27] Z. Liu, Z. Zhen, Z. Zuo, Y. Wu, A. Liu, Q. Yi, W. Li, Probing the catalytic center of porcine aminoacylase 1 by site-directed mutagenesis, homology modeling and substrate docking. J. Biochem 139 (2006) 421–430.
[28] J.C. Gordon, J.B. Myers, T. Folta, V. Shoja, L.S. Heath, A. Onufriev, H++: a server for estimating pKas and adding missing hydrogens to macromolecules. Nucleic Acids Res. 33 (2005) 368–371.
[29] D. Bashford, M. Karplus, pKa's of ionizable groups in proteins: atomic detail from a continuum electrostatic model. Biochemistry 29 (1990) 10219–10225.
[30] R. Anandakrishnan, A. Onufriev, Analysis of basic clustering algorithms for numerical estimation of statistical averages in biomolecules. J. Comput. Biol. 15 (2008) 165–184.
[31] J. Sambrook, D.W. Russel, Molecular Cloning: a Laboratory Manual. Cold Spring HarborLaboratory Press, 2001.
[32] C.T. Chung, S.L. Niemela, R.H. Miller, One-step preparation of competent *Escherichia coli*: transformation and storage of bacterial cells in the same solution. Proc. Natl. Acad. Sci. U.S.A 86 (1989) 2172–2175.
[33] R. Wardenga, F. Hollmann, O. Thum, U. Bornscheuer, Functional expression of porcineaminoacylase 1 in *E. coli* using a codon optimized synthetic gene and molecular chaperones. Appl. Microbiol. Biotechnol. 81 (2008) 721–729.

[34] U.K. Laemmli, Cleavage of structural proteins during the assembly of the head of bacteriophage T4. Nature 227 (1970) 680–685.
[35] T. Giardina, A. Biagini, F. Dalle Ore, E. Ferre, M. Reynier, A. Puigserver, The hog intestinalmucosa acylase I: subcellular localization, isolation, kinetic studies and biological function. Biochimie 79 (1997) 265–273.
[36] R.J. Fox, M.D. Clay, Catalytic effectiveness, a measure of enzyme proficiency for industrial applications. Trends Biotechnol. 27 (2009) 137–140.
[37] A. Durand, T. Giardina, C. Villard, A. Roussel, A. Puigserver, J. Perrier, Rat kidney acylase I: further characterisation and mutation studies on the involvement of Glu 147 in the catalytic process. Biochimie 85 (2003) 953–962.
[38] M. Tollinger, J.D. Forman-Kay, L.E. Kay, Measurement of side-chain carboxyl pKa values of glutamate and aspartate residues in an unfolded protein by multinuclear NMR spectroscopy. J. Am. Chem. Soc. 124 (2002) 5714–5717.
[39] J.E. Nielsen, T.V. Borchert, G. Vriend, The determinants of {alpha}-amylase pH-activity profiles. Protein Eng. 14 (2001) 505–512.
[40] H.A. Lindner, M. Täfler-Naumann, K.-H. Röhm, N-acetylamino acid utilization by kidney aminoacylase-1. Biochimie 90 (2008) 773–780.
[41] D. Heese, S. Berger, K.H. Röhm, Nuclear magnetic relaxation studies of the role of the metalion in Mn2(+)-substituted aminoacylase I. Eur. J. Biochem. 188 (1990) 175–180.
[42] W.L. Delano, The PyMOL molecular graphics system. DeLano Scientific (2002).